Lasing emission of dye-doped cholesteric liquid crystal microdroplet wrapped by polyglycerol in hollow glass microsphere

Chi Zhang (张 弛)[1], **Dongying Fu** (付冬颖)[1], **Chunli Xia** (夏春莉)[1],
Lishuang Yao (姚丽双)[2,3], **Chunlian Lu** (卢春莲)[1], **Weimin Sun** (孙伟民)[1],
and **Yongjun Liu** (刘永军)[1,2,*]

[1]*Key Laboratory of In-fiber Integrated Optics, Ministry of Education, Harbin Engineering University, Harbin 150001, China*
[2]*State Key Laboratory of Applied Optics, Changchun Institute of Optics, Fine Mechanics and Physics, Chinese Academy of Sciences, Changchun 130033, China*
[3]*Department of Physics, College of Science, Shantou University, Shantou 515063, China*
Corresponding author: liuyj@hrbeu.edu.cn

In this Letter, a dye-doped cholesteric liquid crystal (DDCLC)-filled hollow glass microsphere is demonstrated to be a resonator with good temperature response. A diglycerol layer is used to wrap the DDCLCs microdroplet to keep it steady and control its orientation. The whispering gallery mode (WGM) lasing and photonic band gap (PBG) lasing caused by two different mechanisms were obtained under the pump of a pulsed laser, and the temperature response of these two kinds of lasing was studied. For the liquid crystal and chiral material used in this Letter, both the WGM lasing and the PBG lasing have a blue shift in wavelength with increasing temperature.

Keywords: cholesteric liquid crystal; microdroplet; lasing emission; whispering gallery mode.
doi: 10.3788/COL202018.011402.

Liquid crystal (LC), as a special material, has not only the fluidity of liquid but also the anisotropy of crystal. The fluidity makes it easy to combine with optical microcavities, and the anisotropy provides a method to sense some physical quantities by detecting changes of its refractive index[1–4]. Cholesteric LCs (CLCs), also known as chiral nematic LCs, have drawn particular interests in many fields such as optics, medicine, and biology[5–7]. In addition, the unique helical structures of CLCs can act as photonic band gap (PBG), which could be used to generate low-threshold lasing emission by doping fluorescence dyes in the CLCs and optically pumping in an appropriate way[8–10]. When the light travels inside the optical microcavity, the lower external refractive index causes the total internal reflection at the interface so that the light would be limited within the microcavity and resonate along the interface; this kind of resonance mode is known as whispering gallery mode (WGM)[11,12]. The WGM microcavity has advantages of small mode volume and high quality (Q) factor, which causes particular interests from researchers.

The design of WGM resonators mainly depends on the choice of cavity material, which determines the WGM responses to environmental variations. Solid materials are widely used to form WGM microcavities in many researches. Gao *et al.* manufactured a controlled assembly WGM microsphere structure by chemical synthesis, which showed it as highly sensitive to chemical vapors[13]. Scholten *et al.* coated the microring resonator with nanoparticles to manufacture a detector for microscale gas chromatographic vapor analysis[14]. The solid material microcavity has good stability and a very high Q value[15]. However, in order to achieve high Q values, a more complicated manufacturing process is required to obtain a smooth surface. Solid material microcavities have been widely used in various sensing applications, including not only traditional matter sensing but also field sensing[16,17]. Due to the development of microfluidic technology[18], the LC microdroplets and microshells formed by microfluids have been widely used as WGM microcavities in recent researches. Sofi *et al.* studied the effect of the electric field on the ferroelectric LC microdroplets in transparent perfluoropolymer liquid and proposed that the WGM lasing of the dye-doped ferroelectric LC microdroplets is electrically switchable[19]. Lin *et al.* studied lasing modes in CLC microshells made by microfluidics technology and controlled the lasing modes by tuning the gain area and the gain–loss balance[20]. These microcavities are usually formed in a liquid environment to form a smooth surface and stay stable. Although the LC microcavity is very simple to make, and the good sensitivities of the LCs material bring good responses, the liquid environment would lead to large size and poor stability of the device. Our team has also done some researches on LC-based resonators. Yang *et al.* used dye-doped CLCs (DDCLCs) to coat glass microspheres to form a microshell structure and studied the tuning effect of temperature on the WGM and PBG mode lasings from the microshells[21]. Xiong *et al.*

proposed a resonator that integrated dye-doped nematic LCs with a hollow glass microsphere (HGM) resonant cavity and studied the tuning effect of temperature and electric field on the resonator[22]. Based on these, we conducted further research.

In this Letter, we propose and experimentally demonstrate a multilayer microsphere resonator based on DDCLCs. An HGM is used as the outer shell of the resonator to maintain the stability of the internal liquid environment. Inside the shell, there is a layer of diglycerol, which contains a drop of DDCLC microdroplet. The emission spectrum shows that this resonator could behave as two laser modes under the excitation of a single pump source: the photonic band gap mode and the WGM. Further experiments prove that both laser modes can react to the varying temperature, and the lasing behavior can be controlled by changing the thickness of the liquid layer between the DDCLC microdroplet and the optical microcavity. Based on the mechanisms above, we can control the laser modes of this resonator and use this resonator for sensing the temperature.

The CLCs were prepared by mixing about 26 wt.% chiral material (R811, Bayispace, China) with the LC (TEB30A, $n_o = 1.522$ and $n_e = 1.692$; Yongsheng Huatsing, China). About 1 wt.% fluorescent dye 4-dicyanomethylene-2-methyl-(6-4-dimethylaminostryl)-4 H-pyan (DCM, Exciton, America) was doped into the prepared CLCs as the gain medium. The DDCLC mixtures were mixed ultrasonically and heated in an oven at 60°C to ensure that the materials are mixed evenly. The mixture was centrifuged after cooling to room temperature to remove any remaining undissolved solid particles. The fabrication process of the resonator was as follows. (1) A low refractive index HGM ($n = 1.45$, diameters ranging from 20 to 115 μm, K25, Minnesota Mining and Manufacturing Company, America) was first fixed on the end face of a single-mode fiber (SMF) with ultraviolet curing adhesive. (2) A sharp tip fiber, which was fabricated by the fusion splicer, was used to form a 10 μm diameter microhole on the HGM. (3) A 5 μm diameter microtube, which was fabricated by the flame-heated taper-drawing technique and connected to a syringe pump, was used to inject the diglycerol and DDCLCs into the HGM. The diglycerol was injected first, and then the DDCLCs were injected into the diglycerol until the HGM was filled with these two liquids; thereby the DDCLC microdroplet could be wrapped by the diglycerol layer. The diglycerol layer can help the DDCLC microdroplet form the helix structure of the cholesteric phase. So far, we had fabricated the DDCLC microdroplet resonator. The diameter of the DDCLC microdroplet and the thickness of the diglycerol layer could be controlled by changing the injection volume of DDCLCs and diglycerol.

A schematic diagram of the experimental setup is shown in Fig. 1. A frequency doubled neodymium-doped yttrium aluminum garnet (Nd:YAG) pulsed laser (532 nm, 8 ns pulse width, and 5 Hz repetition rate) was used to excite the DDCLC microdroplet resonator. The pump light was
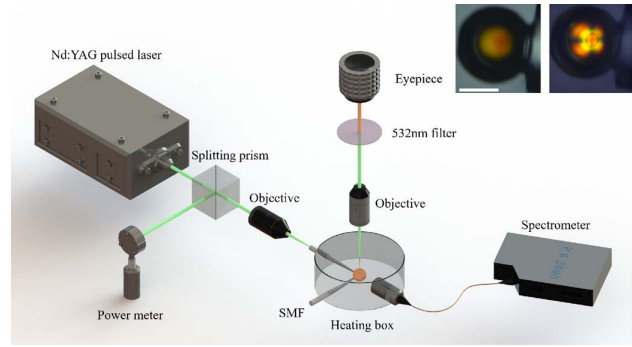

Fig. 1. Schematic diagram of the experimental setup. The insets are the microscopy images of the HGM filled with DDCLCs and a diglycerol layer (the left inset is an unpolarized image, the right inset is an orthogonal polarized image). Scale bar is 50 μm.

split into two beams, one was collected by the optical power meter to monitor the intensity of the excitation light, and the other beam was concentrated by a 10× microscope objective (NA = 0.25) to excite the DDCLC microdroplet. The emission light from the resonator was collected by a fiber optic probe, which was connected to the spectrometer (spectral resolution = 0.01 nm) to obtain the emission spectrum. To study the effect of temperature, we used a heating stage (minimum regulation value of 0.1°C) to vary the surrounding temperature.

Before we finally determined the multilayer structure of the resonator, we studied the lasing behavior of an HGM only filled with DDCLCs. This experiment aimed to verify whether the DDCLCs in the HGM can form good helix structures by only the action of the chiral material. Figure 2(a) shows the emission spectrum of a 67 μm HGM filled with DDCLCs at room temperature; the insets of Fig. 2(a) are microscopy images of the DDCLC-filled HGM. In the inset images, we can see that the pumped DDCLC-filled HGM shows a bright ring at the surface
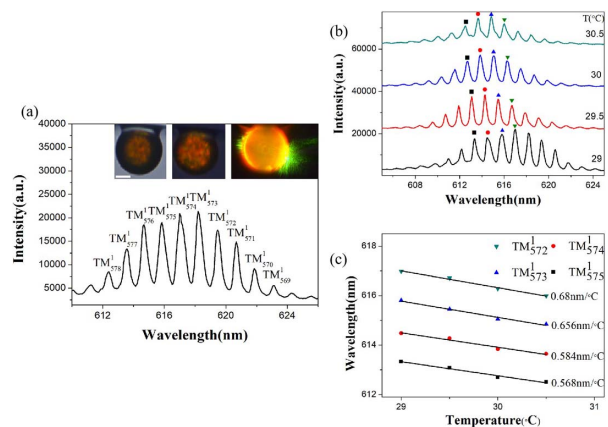

Fig. 2. (a) Emission spectrum of the DDCLC-filled HGM. (b) The emission spectra of the DDCLC-filled HGM as a function of temperature. (c) The wavelength shift of the marked peaks as a function of temperature. The insets of (a) from left to right are, respectively, an unpolarized image, orthogonal polarized image, and excited image of the DDCLC-filled HGM. Scale bar is 20 μm.

of DDCLCs, which is caused by the WGM resonance. In order to distinguish the peaks from each other, we calculated the angular mode numbers l, which can be simply expressed as $l = 2\pi n r/\lambda$, where n is the refractive index of DDCLCs, r is the radius of the DDCLC microdroplet, and λ is the resonance wavelength[23]. The calculated l that belongs to first-order TM modes is marked in Fig. 2(a). Figure 2(b) shows the emission spectra of the DDCLC-filled HGM at different temperatures. It is obvious that the spectrum has a blue shift with the increasing temperature. For a WGM cavity, the change of temperature would change the refractive index and the size of the cavity, and thus causes the change of resonance wavelength. The relationship between the temperature variety and the resonance wavelength can be expressed as follows[24]:

$$\Delta \lambda = \lambda_0 \left(\frac{1}{n} \frac{\mathrm{d}n}{\mathrm{d}T} \Delta T + \frac{1}{D} \frac{\mathrm{d}D}{\mathrm{d}T} \Delta T \right), \qquad (1)$$

where $\mathrm{d}n/\mathrm{d}T$ represents the thermo-optic coefficient, and $D^{-1}\mathrm{d}D/\mathrm{d}T$ represents the thermal expansion coefficient. Considering the limitations of the HGM to the volume of inside liquids, the volume of the DDCLC microdroplet would hardly change with the change of temperature, which means the change of emission spectrum is mainly caused by the refractive index change of DDCLCs. Since there are only TM modes in the emission spectra, the refractive index n in Eq. (1) can be considered as the extraordinary refractive index n_e of DDCLCs, and its relationship with temperature can be expressed by the following equation[25]:

$$\frac{\mathrm{d}n_e}{\mathrm{d}T} = -B - \frac{2\beta(\Delta n)_o}{3\,T_c(1 - \frac{T}{T_c})^{1-\beta}}, \qquad (2)$$

where B is a constant determined by the material, β is an exponent, T_c is the clear temperature of the LC material, and $\Delta n = n_e - n_o$. For the LC material in our experiment, the value of $\mathrm{d}n_e/\mathrm{d}T$ is negative, and thus the increase of temperature will cause a decrease of the DDCLC's refractive index and thereby cause the blue shift of the WGM resonance wavelength. We have calculated the temperature sensitivity of the four peaks marked in Fig. 2(b). As shown in Fig. 2(c), all these peaks have blue shift in wavelengths when the temperature rises.

Unfortunately, the PBG mode lasing was not observed from this kind of DDCLC-filled HGM, which means that the DDCLCs in the HGM could not form good helix structures. Therefore, we improved the resonator structure to try to obtain the WGM resonance lasing and the PBG mode lasing at the same time.

In order to obtain the PBG lasing from the resonator, we have made some attempts. It was found that the glycerol would help the DDCLCs to form helix structures[26]. Therefore, we tried to inject glycerol into the HGM and let the DDCLC microdroplet be covered by the glycerol. In this process, we found that the viscosity of this liquid is

too low to keep the DDCLC microdroplet steady, so we used diglycerol to replace glycerol. They have similar molecular structures, but the diglycerol is more viscous. The emission spectrum of a well-formed DDCLC microdroplet resonator (the diameter of the DDCLC microdroplet is about 60 μm) is shown in Fig. 3(a). The left inset is the image of the resonator under the polarizing microscope; the unique figure of the DDCLC microdroplet shows the formation of the helix structure. The right inset shows the resonator under the pump of a 532 nm laser; the bright spot in the center of the DDCLCs microdroplet is the PBG mode lasing, while the ring at the surface of the DDCLCs is the WGM lasing. In this spectrum, it would be easy to identify two different modes of the laser. The single peak with high intensity is the PBG mode lasing, while the periodic peaks with lower intensities are the WGM lasing. From this spectrum, we obtained that the resonance line widths ($\Delta\lambda$) of the PBG mode lasing and the WGM lasing are, respectively, 0.34 nm and 0.14 nm. The Q factors can be calculated by the formula $Q = \lambda/\Delta\lambda$. The Q factor of PBG mode lasing is about 1.9×10^3, and the Q factor of WGM lasing is about 4.3×10^3.

In addition, in order to study the properties of these two emission modes, some further experiments were carried out. We measured the WGM emission spectra of resonators with different DDCLC microdroplet diameters at the same room temperature, as shown in Fig. 3(b). According to the formula $\mathrm{FSR} = \lambda^2/(\pi n_{\mathrm{eff}} D)$, in which λ is the resonance wavelength, and n_{eff} is effective refractive index, we can know that the free spectral range (FSR) of the WGM resonance is inversely proportional to the WGM resonant cavity diameter D[27]. The experimental data also proves this: at room temperature, the FSRs of the WGM lasing in the resonators with DDCLC microdroplet diameters of 40, 50, and 60 μm are 1.73, 1.55, and 1.38 nm, respectively. The size of the resonant cavity determines the emission wavelengths of the WGMs, but its effect on the emission wavelength of the PBG mode is insignificant. According to the formula $\lambda = n_e p$, the emission wavelength λ of the PBG mode is proportional to the extraordinary refractive index n_e and the helix pitch p of the DDCLCs. The changes in the concentration of the chiral agent in the DDCLCs would cause the changes of the helix pitch
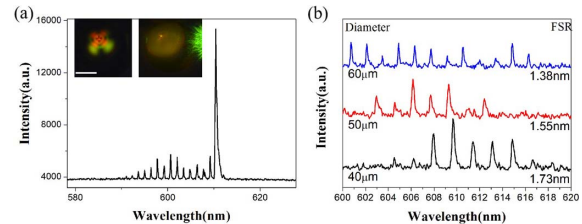

Fig. 3. (a) Emission spectrum of a resonator with a well-formed 60 μm diameter DDCLC microdroplet. (b) The relationship between the diameter of DDCLC microdroplet and the FSR of the WGM peaks. The insets of (a) are, respectively, an orthogonal polarized image and an excited image of the resonator. Scale bar is 30 μm.

and therefore change the emission wavelength of the PBG mode. Based on the above principles, the emission wavelength of the PBG mode and the FSR of WGMs can be adjusted according to the actual needs.

Figure 4(a) shows emission spectra of a resonator under different pump intensities. Figures 4(b) and 4(c) show the thresholds of the PBG mode lasing and the WGM lasing, respectively. When the pump intensity was below the threshold, only the weak and broad spontaneous emission was observed, and the emission intensity growth was slow. Once the pump intensity was above the threshold, the corresponding lasing mode appeared, and the emission intensity increased rapidly with the increasing pump intensity. The threshold of PBG mode lasing is about 7.5 μJ, and the threshold of WGM lasing is about 12.4 μJ. Since the light needs to travel a few circles along the surface of LC microdroplets to form the WGM resonance, the high scattering of LCs and the long optical path in this process will cause a high loss, which could explain the higher threshold of WGM lasing.

Due to the effect of temperature on the refractive index of LC, which would cause wavelength shifts of WGM lasing and PBG mode lasing, it is a feasible way to realize the tuning of wavelength or the sensing of temperature. The pump intensity was set slightly above the threshold of the WGMs to excite the PBG mode lasing and the WGM lasing at the same time. The emission spectra of a resonator with a 45 μm DDCLC microdroplet are shown in Fig. 5(a). As the temperature increased, the blue shift of the wavelengths was observed in both the WGMs and the PBG mode. The effect of temperature on WGM lasing has been elucidated above; as temperature rises, the effective refractive index of DDCLCs decreases and thereby causes the blue shift of WGM resonance wavelength. From the equation $\lambda = n_e p$, the wavelength λ of PBG mode lasing is determined by the extraordinary refractive index n_e and the helix pitch p of DDCLCs. According to Eq. (2), n_e of TEB30A would decrease with the increasing temperature. The effect of temperature on the helix pitch p is affected by the choice of LCs and chiral material[28]. Thus, for the materials selected in our experiments, the wavelength of PBG mode lasing would have a blue shift as the

Fig. 5. (a) Emission spectra of a resonator with a 45 μm DDCLC microdroplet. (b) The wavelength shift of the marked WGM peak as the temperature increases. (c) The wavelength shift of the PBG mode peak as the temperature increases.

temperature increases. Figure 5(b) shows the relationship between the temperature and the wavelength of a WGM peak, which is marked in Fig. 5(a). Figure 5(c) shows the relationship between the temperature and the PBG mode wavelength. It is clear that both the WGMs and the PBG mode have linear responses to temperature changes. When the temperature increased from 29°C to 31.6°C, the wavelength of WGMs had a blue shift of 7.75 nm, and the wavelength of the PBG mode shifted from 594.88 nm to 589.16 nm, which, respectively, corresponded to sensitivities of 2.98 nm/°C and 2.2 nm/°C. Compared with the resonator without diglycerol, the resonator with diglycerol has a much higher sensitivity for WGM lasing. Moreover, the sensitivity difference between the WGM lasing and PBG mode lasing may bring a possibility of multiparameter sensing.

When the DDCLCs were injected into the diglycerol layer, it was hard to control the position of the formed microdroplet. In other words, the formed microdroplet might not be exactly in the center of the diglycerol but be close to one side, just as the inset in Fig. 3 shows. In order to confirm the effect of the microdroplet position on the performance of the resonator, some further experiments were carried out. A resonator was excited at different positions on the same plane, as the inset in Fig. 6 shows. The corresponding excitation spectra are shown in Fig. 6.
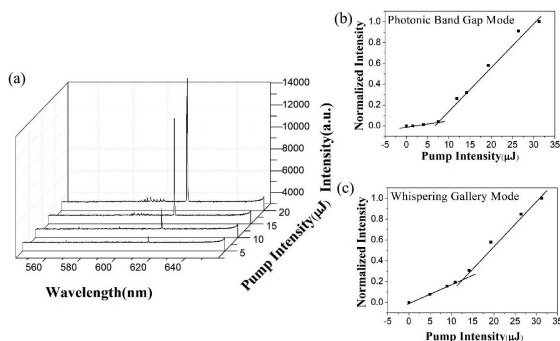
Fig. 4. (a) Emission spectra of a resonator under different pump intensities. (b) Normalized threshold curve of PBG mode lasing. (c) Normalized threshold curve of WGM lasing.
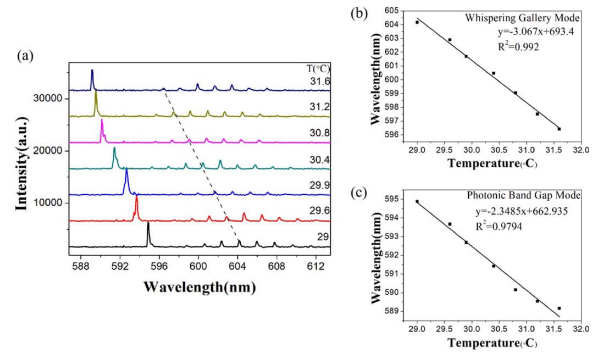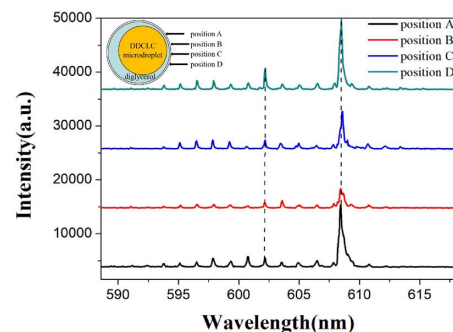
Fig. 6. Emission spectra of a resonator excited at different positions. The inset is the schematic diagram of the excitation positions.

The different positions of excitation are equivalent to different relative positions between the microdroplet and the HGM; thus, we could confirm the effect of the microdroplet position by the spectra in Fig. 6. Since the spectra in Fig. 6 are almost identical, it can be considered that the microdroplet position has almost no effect on the spectrum.

In conclusion, a resonator based on DDCLC microdroplets is proved. In the experiment of the resonator, which has only DDCLCs in the HGM, only the WGM lasing is obtained, which means that the DDCLCs could not form a helix structure by itself. Then, a diglycerol layer is used to wrap the DDCLC microdroplet to control its orientation; then WGM lasing and the PBG mode lasing can be obtained from the resonator at the same time under a pulsed laser pump. The experiment on the microdroplet size shows that the diameter of DDCLCs microdroplets would determine the FSR of the WGM lasing. Additionally, the temperature responses of the WGM lasing and the PBG mode lasing have been studied. For the resonator without diglycerol, the WGMs have a sensitivity of 0.68 nm/°C. For the resonator with diglycerol, the WGMs can reach a sensitivity of 2.98 nm/°C, and the PBG modes can reach a sensitivity of 2.2 nm/°C. This may provide the possibility of highly sensitive temperature sensing and thermally tunable microlasers in the air environment.

References
1. C. Yang, H. Zhang, B. Liu, S. Lin, Y. Li, and H. Liu, Opt. Lett. **42**, 2988 (2017).
2. M. Humar and I. Musevic, Opt. Express **19**, 19836 (2011).
3. C. R. Smith, D. R. Sabatino, and T. J. Praisner, Exp. Fluids **30**, 190 (2001).
4. Z. Zhang, H. Xu, H. Yang, Z. You, and D. P. Chu, Chin. Opt. Lett. **14**, 111601 (2016).
5. H. Jing, Y. Xiang, M. Xu, E. Wang, J. Wang, N. Eber, and A. Buka, Phys. Rev. Appl. **10**, 014028 (2018).
6. M. Schwartz, G. Lenzini, Y. Geng, P. B. Ronne, P. Y. A. Ryan, and J. P. F. Lagerwall, Adv. Mater. **30**, 1707382 (2018).
7. K. Kek, J. Lee, Y. Otono, and S. Ishihara, J. SID **25**, 366 (2017).
8. W. Li, C. Yang, B. Luo, Z. Wang, X. Wang, Y. Bu, S. Li, H. Xu, and L. Chen, Chin. Opt. Lett. **12**, 111602 (2014).
9. C. Lee, J. Lin, B. Huang, S. Lin, T. Mo, S. Huang, C. Kuo, and H. Yeh, Opt. Express **19**, 2391 (2011).
10. J. Lin, M. Hsieh, G. Wei, T. Mo, S. Huang, and C. Lee, Opt. Express **21**, 15765 (2013).
11. L. Zheng, M. Zhi, Y. Chan, and S. A. Khan, Sci. Rep. **8**, 14088 (2018).
12. M. Wang, X. Jin, F. Li, B. Cai, and K. Wang, Opt. Commun. **427**, 70 (2018).
13. M. Gao, C. Wei, X. Lin, Y. Liu, F. Hu, and Y. Zhao, Chem. Commun. **53**, 3102 (2017).
14. K. Scholten, W. R. Collin, X. Fan, and E. T. Zellers, Nanoscale **7**, 9282 (2015).
15. X. Jiang, L. Shao, S. Zhang, X. Yi, J. Wiersig, L. Wang, Q. Gong, M. Loncar, L. Yang, and Y. Xiao, Science **358**, 344 (2017).
16. X. Jiang, A. J. Qavi, S. H. Huang, and L. Yang, "Whispering gallery microsensors: a review," https://arxiv.org/abs/1805.00062 (2018).
17. X. Jiang, C. Zou, L. Wang, Q. Gong, and Y. Xiao, Laser Photon. Rev. **10**, 40 (2016).
18. M. Chen, W. Jia, J. He, M. Geiser, and G. Zheng, Chin. Opt. Lett. **17**, 041201 (2019).
19. J. A. Sofi and S. Dhara, Appl. Phys. Lett. **114**, 091106 (2019).
20. Y. Lin, L. Gong, K. Che, S. Li, C. Chu, Z. Cai, C. Yang, and L. Chen, Appl. Phys. Lett. **110**, 223301 (2017).
21. Y. Lu, Y. Yang, Y. Wang, L. Wang, J. Ma, L. Zhang, W. Sun, and Y. Liu, Opt. Express **26**, 3277 (2018).
22. Z. Xiong, C. Zhang, J. Hu, D Fu, Y. Lu, W. Sun, and Y. Liu, Appl. Phys. Express **12**, 022003 (2019).
23. S. K. Y. Tang, R. Derda, Q. Quan, M. Lončar, and G. M. Whitesides, Opt. Express **19**, 2204 (2011).
24. C. H. Dong, L. He, Y. F. Xiao, V. R. Gaddam, S. K. Ozdemir, Z. F. Han, G. C. Guo, and L. Yang, Appl. Phys. Lett. **94**, 231119 (2009).
25. J. Li, S. Gauzia, and S.-T. Wu, Opt. Express **12**, 2002 (2004).
26. M. Humar, F. Araoka, H. Takezoe, and I. Musevic, Opt. Express **24**, 19237 (2016).
27. R. Chen, V. D. Ta, and H. Sun, ACS Photon. **1**, 11 (2014).
28. M. F. Moreira, I. C. S. Carvalhoa, W. Cao, C. Bailey, B. Taheri, and P. P. Muhoray, Appl. Phys. Lett. **85**, 2691 (2004).